



ELSEVIER

Available online at www.sciencedirect.com

SCIENCE @ DIRECT®

Earth and Planetary Science Letters 6786 (2003) 1–14

EPSL

www.elsevier.com/locate/epsl

Non-dipole fields and inclination bias: insights from a random walk analysis

Joseph G. Meert*, Endale Tamrat, John Spearman

Department of Geological Sciences, University of Florida, 241 Williamson Hall, Gainesville, FL 32611, USA

Received 25 April 2003; received in revised form 9 July 2003; accepted 18 July 2003

Abstract

The paleomagnetic assumption that the Earth's magnetic field is reduced to a geocentric axial dipole (GAD) when sufficiently sampled has been called into question for Mesozoic and earlier times. It has been suggested, for example, that modest contributions from axial quadrupolar (10%) and octupolar (25%) fields are resolvable using inclination only data from paleomagnetic studies. The underlying assumption in inclination only studies is that considerable continental drift has occurred over a sufficiently long period of time to render paleomagnetic sampling random in a paleogeographic sense. This assumption was stated in all previous studies dating back to 1976, but was never tested. We have developed a random walk model designed to test this assumption. Our model uses three different configurations for the continents in the random walk and allows the user to vary parameters such as maximum velocity, sampling distribution, sampling frequency and frequency of directional change. The model generates large sample sizes that cannot be adequately evaluated using the standard χ^2 statistical test and therefore we introduce two statistical parameters used in structural equation models. Our models indicate that the 'random paleogeographic sampling' assumption used in the previous studies is not valid due primarily to the lack of an adequate sample size and temporal distribution. We show, for example, that even the most robust dataset compiled in 1998 is severely undersampled. A series of model runs on a GAD earth with sampling over a 600 Myr period demonstrates that detailed sampling will, on average, produce a GAD-like distribution only 30% of the time. Other model runs demonstrate that inadequate sampling can produce false quadrupolar and octupolar effects. It is our conclusion that time-averaged inclination only studies using the extant paleomagnetic database should be viewed with extreme caution.

© 2003 Published by Elsevier B.V.

Keywords: geocentric axial dipole; octupole; quadrupole; paleomagnetism; inclination

1. Introduction

One of the fundamental working assumptions

in paleomagnetic studies is that the Earth's magnetic field averages to a geocentric axial dipole (GAD) when sufficiently sampled. While the assumption seems to hold, within error, for the past 5 million years [1,2], it has been recently questioned for pre-Mesozoic times [3–5]. It has been suggested, for example, that contributions from axial quadrupolar (10%) and octupolar (25%)

* Corresponding author.

E-mail address: jmeert@geology.ufl.edu (J.G. Meert).

40 fields are resolvable using inclination only data
 41 from paleomagnetic studies on Precambrian and
 42 Paleozoic datasets [3]. Others [4,5] have analyzed
 43 perceived misfits between continental reconstruc-
 44 tions and paleomagnetic data and suggested a
 45 modest contribution from a persistent (e.g. 10%)
 46 octupolar field during Paleozoic and Mesozoic
 47 time. Because persistent non-dipole fields can
 48 cause errors in paleomagnetically based recon-
 49 structions, it is important to develop several reli-
 50 able independent tests for the GAD assumption.

51 Evans [6] proposed one such test that relies
 52 solely on the frequency of inclination data
 53 through time. He argued that a ~ 600 Myr ran-
 54 dom cycling of continents around the globe
 55 should produce a distribution of magnetic inclina-
 56 tions that follows a probability function based on
 57 the surface area occupied by the sampling sites
 58 over time. This probability function is easily
 59 solved by estimating the surface area of the globe
 60 corresponding to any set of inclination classes
 61 (typically 10° intervals). In an effort to minimize
 62 sample bias problems, the inclination data are
 63 binned in $10^\circ \times 10^\circ$ grids for a given time interval
 64 [3,6]. The surface area of the globe corresponding
 65 to each inclination class can be calculated by:

$$66 \quad \partial\Omega = 2\pi \int_{\phi_1}^{\phi_2} \sin\phi \partial\phi \quad (1)$$

67 where ϕ is the co-latitudinal range corresponding
 68 to each inclination class. Assuming a GAD field,
 69 Eq. 1 should produce the inclination frequency
 70 distribution shown in Fig. 1. The dependence of
 71 the absolute value of the inclination $|I|$ on co-
 72 latitude (ϕ) for axial multipoles is given by:

$$73 \quad \tan I_l = \frac{-(1+I)P_l}{(\partial P_l / \partial \phi)} \quad (2)$$

74 where P_l is the Legendre polynomial of degree l
 75 and I_l is the resulting inclination from the axial
 76 multipole of degree l . The solution to Eq. 2 for
 77 axial quadrupolar ($G2 = g_0^2/g_1^0$) and octupolar
 78 ($G3 = g_0^3/g_1^0$) fields is given by [6] as:

$$79 \quad \tan I' = \frac{2\cos\phi + 1.5 \times G2(3\cos^2\phi - 1) + 2 \times G3(5\cos^3\phi - 3\cos\phi)}{\sin\phi + G2(3\sin\phi\cos\phi) + 1.5 \times G3(5\sin\phi\cos^2\phi - \sin\phi)} \quad (3)$$

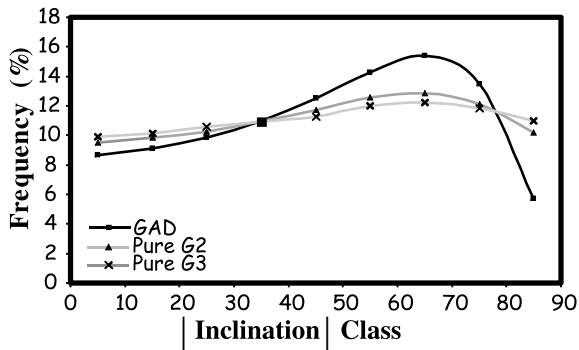
80 Eq. 3 can be used to compare observed inclina-
 81 tion frequencies with expected inclination fre-

quencies based on various contributions of non-
 dipole fields (Fig. 1). The original analysis found
 that inclination only data were compatible with
 the GAD hypothesis at least for the last 600 mil-
 lion years [6]. Subsequent studies [3,7] reached
 different conclusions. Piper and Grant [7], using
 unbinned inclination data, concluded that the ob-
 served inclination frequencies were compatible
 with the GAD assumption for the time interval
 from 600 to 3000 Ma, but were significantly dif-
 ferent than GAD for the time interval from 300 to
 600 Ma. Kent and Smethurst [3], using binned
 data, concluded that the GAD hypothesis could
 not be rejected for the Mesozoic and Cenozoic,
 but the observed distributions were significantly
 different (at the 95% confidence level) from
 GAD during the Paleozoic and Precambrian.

There were a number of explanations offered
 for this departure from GAD. For example,
 [3,5,8] suggested that stabilization of the inner
 core, via growth, might stabilize the geodynamo
 and result in diminishing contributions from high-
 er order harmonics through time. Inclination shal-
 lowing was also proposed to explain the apparent
 bias towards low inclinations [3,5]. This explana-
 tion appears less likely because the inclination
 bias is also observed in igneous rocks [3,5]. Other
 explanations include preferential cycling of conti-
 nents to low latitudes via true polar wander [3,7];
 the indiscriminate use of poorly resolved paleo-
 magnetic data [9] or that the underlying assump-
 tion of random sampling of the globe is invalid
 [9].

Evans [6], in his original analysis of inclination
 only data, asserted that the last 500–600 million
 years of continental drift rendered the paleomag-
 netic sampling random in a paleogeographic
 sense. Subsequent studies [3,7] made a similar
 ‘random sampling’ assertion, but provided no evi-
 dence to support the assumption. In addition,
 both [3] and [7] made a fundamental error in their
 calculation of the χ^2 value. In this paper, we ex-
 amine the underlying assumption of random sam-
 pling and provide a more sensitive test of signifi-
 cance for the observed distributions.

82
83
84
85
86
87
88
89
90
91
92
93
94
95
96
97
98
99
100
101
102
103
104
105
106
107
108
109
110
111
112
113
114
115
116
117
118
119
120
121
122
123
124
125
126



1 Fig. 1. Theoretical inclination class frequency curves for a
 2 GAD field, a pure G2 (quadrupole) field and a pure G3 (oc-
 3 tupole field).

127 2. Previous studies

128 Table 1 shows the results of previous studies on
 129 inclination only data from the paleomagnetic da-
 130 tabase. Each of these studies applied the χ^2 test
 131 (see Appendix 1a) to the observed and theoretical
 132 distributions. We note, however, that the studies
 133 of [3,7] incorrectly applied the χ^2 test resulting in
 134 an underestimate of the χ^2 value (see Table 1 for
 135 corrected values). This underestimate significantly
 136 affects the conclusions of [7] regarding the Phan-
 137 erozoic and Precambrian datasets. The original
 138 paper concluded that the observed distributions
 139 were indistinguishable from GAD; however, the

140 corrected χ^2 values indicate that the two distribu-
 141 tions are significantly different from GAD above
 142 the 99% confidence interval (99% $\chi_{crit}^2 = 20.09$). In
 143 the case of [3], the corrected χ^2 values render the
 144 Mesozoic distribution different than the GAD
 145 above the 99% confidence interval (Table 1).
 146 The other χ^2 values cited in [3] also increase,
 147 but the conclusions remain identical to the pre-
 148 vious study, namely that the Paleozoic and Pre-
 149 cambrian data are significantly non-GAD.

150 We were initially interested in extracting the
 151 temporal development of the non-GAD field
 152 from the paleomagnetic inclination database.
 153 Therefore, we developed an algorithm that can
 154 take the measured inclination distribution and in-
 155 vert Eq. 3 to generate a family of ‘best-fit’ solu-
 156 tions based on varying contributions of the G2
 157 (quadrupolar) and G3 (octupolar) fields and the
 158 calculated χ^2 value. Thus, if the assumption of
 159 random sampling has been met and the χ^2 test
 160 statistic is a valid measure of goodness of fit,
 161 then these families of G2 and G3 contributions
 162 might provide information regarding the evolu-
 163 tionary development of the magnetic field through
 164 time. Table 1 lists the results of this analysis for
 165 the previous studies. Although the relative contri-
 166 butions of G2 and G3 vary over time according to
 167 the analysis conducted by [3], there appears to be
 168 no systematic change evident in their relative con-
 169 tributions on a temporal scale. This led us to seek

Table 1
 Previous results

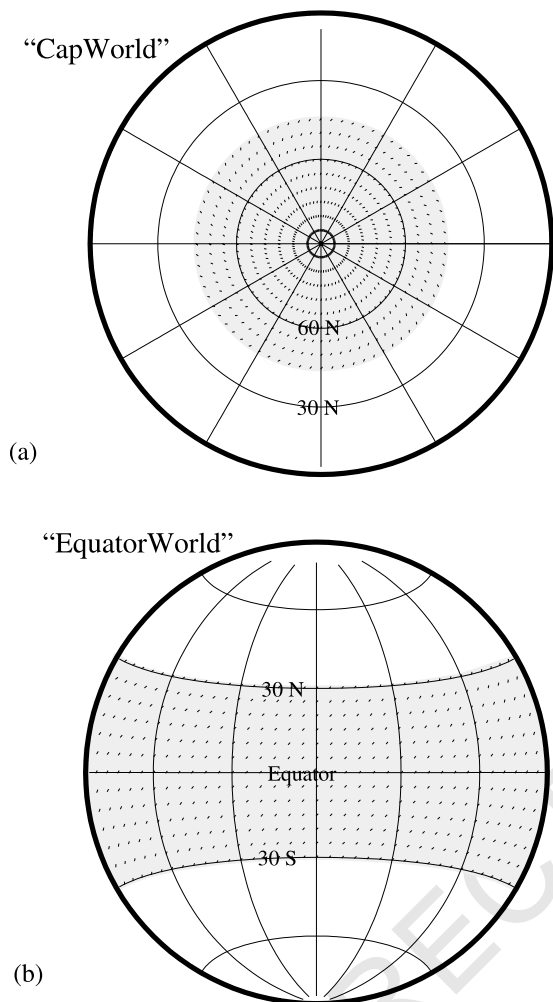
1	Period	Bins or observations	Reference	χ_1^2	χ_2^2	N_{crit}	RMSEA	G2	G3
2	Cambrian–Tertiary	430	[6]	13.49	13.49	494.2	0.07	NC	NC
3	Phanerozoic (0–600 Ma)	3888 ^a	[7]	4.61	293.9	206.1	0.10	0.21	0.18
4	Precambrian (600–3000 Ma)	899 ^a	[7]	8.32	136.4	103.1	0.15	0.16	0.22
5	Cenozoic (0–65 Ma)	253	[3]	3.63	9.19	426.3	0.07	NC	NC
6	Mesozoic (65–250 Ma)	342	[3]	7.18	24.50	216.9	0.10	0.28 ^b	0.14 ^b
7	Paleozoic (250–550 Ma)	352	[3]	32.23	113.48	48.9	0.21	0.11	0.28
8	Precambrian (550–3500 Ma)	531	[3]	20.39	108.76	76.6	0.17	0.14	0.23
9	All (0–3500 Ma)	1478	[3]	–	135.75	169.8	0.11	0.16	0.17
10	Phanerozoic	947	[3]	–	54.33	270.8	0.091	0.18	0.14
11	Mesozoic+Cenozoic	595	[3]	–	28.72	321	0.083	0.31	0.16

12 χ_1^2 , as calculated by the original authors; χ_2^2 as calculated by Meert et al. (this study).

13 N_{crit} = critical N-index or Hoelster index; RMSEA = root mean square error of approximation; G2 and G3 are best-fit calculation
 14 to the observed binned distribution; NC = not calculated since the results are indistinguishable from GAD.

15 ^a Not binned.

16 ^b Best fit is still significantly different than both GAD and the observed distribution at the 95% confidence level using the χ^2
 17 test.



1 Fig. 2. (a) ‘Cap world’ continent representing $\sim 11\%$ of the
 2 Earth’s surface area. Sampling sites (dots) are located at 5°
 3 intervals. (b) ‘Equator world’ continent representing $\sim 25\%$
 4 of the Earth’s surface area. Sampling sites (dots) are located
 5 at 5° intervals.

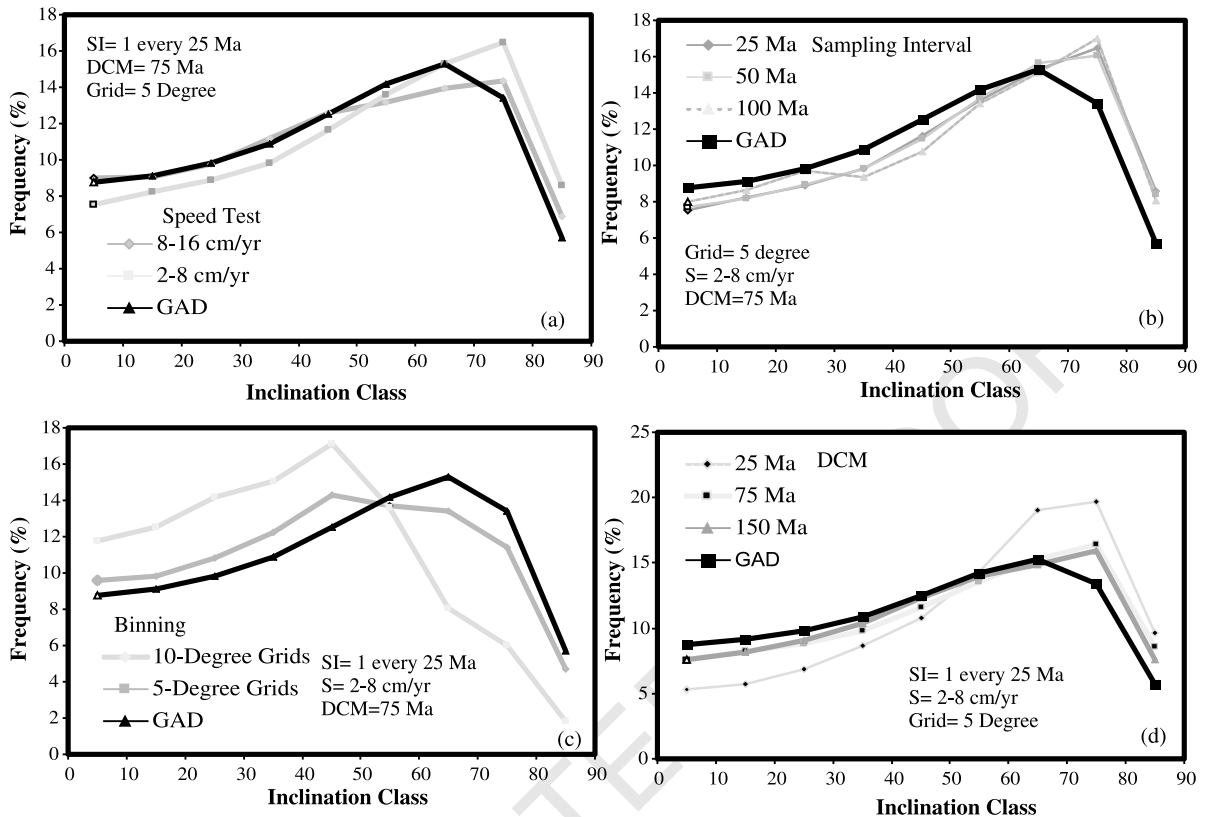
170 an alternative explanation for the non-GAD dis-
 171 tributions cited by [3].

172 3. A random walk model

173 The basic assumption inherent in each of the
 174 three previous inclination only studies [3,6,7]
 175 was that 500–600 million years is enough time
 176 to randomly sample the globe. This assumption
 177 has never been tested. We formulated an algo-

178 rithm for generating a continental-size random
 179 walk on a sphere. In an effort to accurately sim-
 180 ulate continental drift, we have generated different
 181 continental configurations. One configuration is
 182 based on the present-day geography of the earth
 183 (major continents only) with ‘sampling’ locations
 184 positioned at 5° intervals. This is equivalent to
 185 binning the observations as suggested by [3,6] us-
 186 ing 5° bins instead of 10° bins. Other configura-
 187 tions used in this analysis were an ‘equator world’
 188 starting configuration (Fig. 2b) and a ‘cap world’
 189 starting configuration (Fig. 2a). In order to simu-
 190 late both the rotational and translational compo-
 191 nents of motion, each continent is rotated about a
 192 computer-generated random Euler pole (see Ap-
 193 pendix 1b). Since the maximum velocity of any
 194 point on the continent is dependent on its distance
 195 from the Euler pole, maximum drift velocities
 196 were constrained to between 2 and 8 cm/yr via a
 197 random number generator. This method of con-
 198 trolling velocity has the practical effect of produc-
 199 ing continental motion with variable drift rates.
 200 We also analyzed the major directional changes
 201 evident in the Phanerozoic apparent polar wander
 202 path for Laurentia. The path indicates a major
 203 directional change approximately every 75 Myr
 204 on average. For most of our models, we used a
 205 75 Myr time period as the interval of constant
 206 motion. The algorithm thus generated a new Euler
 207 pole and velocity maximum every 75 Myr.
 208 Each of these parameters is user controlled.
 209 Lastly, the algorithm allows the user to ‘sample’
 210 the GAD field at a given frequency. Most of our
 211 runs collected an inclination sample at each site
 212 for every 25–50 million years. The total duration
 213 of each run lasted 575 Myr, 600 Myr or 3500
 214 Myr. The computer program calculates the χ^2
 215 test statistic, the Hoelter index (or N_{crit} value)
 216 and the root mean square error of approximation
 217 (or RMSEA; see Appendix 1a) after each sam-
 218 pling period. We consider a good fit to the theo-
 219 retical distribution reached when two of the three
 220 statistical measures fall within the critical values
 221 ([11,14]; χ^2 value < 15.51 ; RMSEA < 0.05 ;
 222 $N_{\text{crit}} > 200$).

223 We ran a number of sensitivity tests on the
 224 model as shown in Fig. 3. In general, the models
 225 are relatively insensitive to speed (S) and sampling

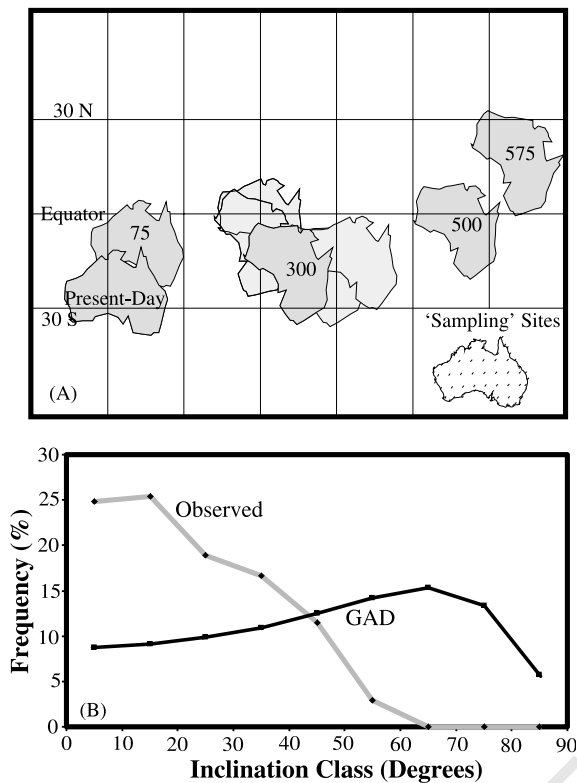


1 Fig. 3. Model sensitivity tests showing (a) a 575 Myr run of 'today world'. Each of these runs started with the same random
 2 seed value. (a) Sensitivity of the model to changing drift rates. After 575 Myr, the 'faster' drift rates results in a slightly improved
 3 fit, but the two curves are not statistically different. (b) A 575 Myr run of 'today world' using different sampling intervals (1
 4 sample every 25 Myr, 1 sample every 50 Myr or 1 sample every 100 Myr). The 1/25 and 1/50 Myr runs are almost identical. The
 5 1/100 Myr sampling interval results in only a slightly more uneven distribution of inclination values. (c) A 575 Myr run of 'equator
 6 world' using a $5^\circ \times 5^\circ$ grid and a $10^\circ \times 10^\circ$ grid. The $10^\circ \times 10^\circ$ grid results in a significant loss of signal with respect to the
 7 $5^\circ \times 5^\circ$ grid. (d) A 575 Myr run of 'today world' demonstrating the sensitivity of the model to changing the direction of plate
 8 motion. The model appears to be more sensitive to rapid directional changes (e.g. 1 every 25 Myr) as compared to slower plate
 9 motion changes (e.g. 1 every 75–150 Myr).

226 interval (SI; within the ranges shown in Fig. 3a,b)
 227 and most sensitive to the gridding interval (Fig.
 228 3c) and the duration of constant motion (DCM;
 229 Fig. 3d). It is possible to choose extreme values
 230 for any of these parameters and drastically change
 231 the results; however, we have attempted to run
 232 the model within the confines of reasonable geo-
 233 dynamic conditions as described above.

234 Since it is difficult to illustrate 3500 million
 235 years of drift on the globe, we chose to illustrate
 236 the mechanics of the model using a synthetic drift
 237 history of Australia over a 600 million year period
 238 (Fig. 4A,B). The model begins with Australia in

239 its present-day position. In this run, the assigned
 240 model parameters included maximum drift rates
 241 of 2–8 cm/yr, sample collection every 25 million
 242 years and directional change every 75 Myr. The
 243 results of this particular model run show that
 244 Australia was restricted to latitudes between
 245 30°N and 30°S . Most of the sampled units should
 246 therefore generate inclinations of less than 50° .
 247 The observed frequency distribution is shown in
 248 Fig. 4B in agreement with the modeled drift his-
 249 tory.



1 Fig. 4. (A) Synthetic drift history of Australia during a 575
 2 Myr model run. The starting point was the present-day position
 3 of Australia. The inset shows the sampling locations
 4 within Australia. (B) Observed inclination class–frequency di-
 5 agram based on the drift in A.

250 4. Results

251 4.1. Cap world

252 This model was run using a continental spher-
 253 ical cap. The SI was 25 Ma, S varied between 2
 254 and 8 cm/yr and DCM was 75 Myr. This model,
 255 representing 11.7% of the surface area on the
 256 Earth, illustrates several key observations regard-
 257 ing the random drift assumption and the sensitiv-
 258 ity of the χ^2 test statistic. The statistical results of
 259 this run are shown in Fig. 5. Fig. 5a shows the
 260 value for each of the three test statistics after each
 261 25 Myr sampling interval. Although N_{crit} rises
 262 above 200 after 875 Ma, it is not until 1475 Ma
 263 that both the RMSEA and N_{crit} reach critical val-
 264 ues (Fig. 5b, Table 2). The ‘best fit’ is achieved
 265 after 2050 Myr.

266 4.2. Equator world

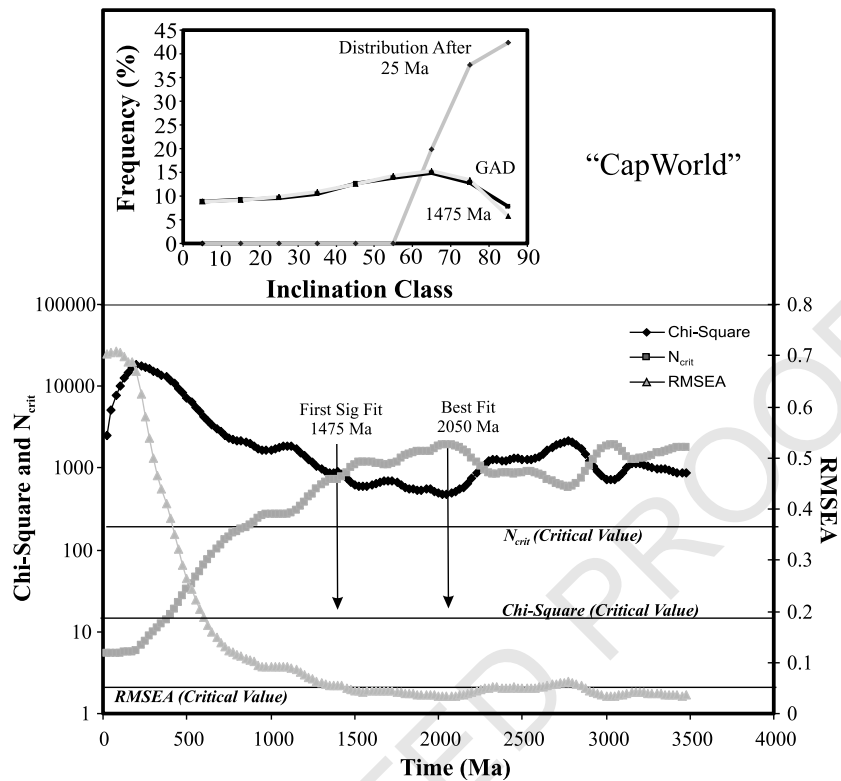
267 This model was run using a hemispheric equa-
 268 torial continent. The SI, S and directional change
 269 DCM were equivalent to the cap world model
 270 described above. The model represents 25% of
 271 the Earth and thus serves as a reasonable proxy
 272 for the current land surface of the Earth. The
 273 statistical results of this run are shown in Fig. 6.
 274 In this case, a ‘good fit’ is first reached at 600 Myr
 275 (Fig. 6a), and much better statistical fits were
 276 achieved at 750 Myr and again at 1200 Myr.
 277 The latter two results fell within the critical inter-
 278 vals for all three statistical measures (Fig. 6a, Ta-
 279 ble 2). The model run at 750 Myr shows the effect
 280 of calculating the Hoelter index when the χ^2 test
 281 statistic is not significant. In this case, N_{crit} has a
 282 value exceeding the number of samples in the
 283 population (Table 2).

284 4.3. Today world

285 This model uses the present-day distribution of
 286 the major continents as a starting point. The SI, S
 287 and DCM were equivalent to the cap world and
 288 equator world models described above. The sta-
 289 tistical results of this run are shown in Fig. 7 and
 290 listed in Table 2. The model reached a good fit
 291 after 725 Myr and a best fit at 1125 Myr.

292 4.4. Runs at 600 Myr

293 Evans [6] argued that 500–600 Myr of continen-
 294 tal motion is sufficient to produce a random geo-
 295 graphic sampling of paleomagnetic data. In order
 296 to test this assertion, we conducted numerous
 297 tests of the random walk covering 600 Myr (see
 298 Table 2). The models showed a highly variable
 299 response under identical sampling conditions. In
 300 these runs, the sampling interval was taken as 1
 301 sample/25 Myr, the speed was allowed to vary
 302 between maxima of 2 and 8 cm/yr and a direc-
 303 tional change took place every 75 Myr. Fig. 8a,b
 304 shows the results for cap world. In this run, the
 305 model never reaches a statistically valid fit to the
 306 GAD model (Fig. 8a) and the ‘best fit’, obtained
 307 after 600 Myr shows a high inclination bias (Fig.
 308 8b, Table 2).

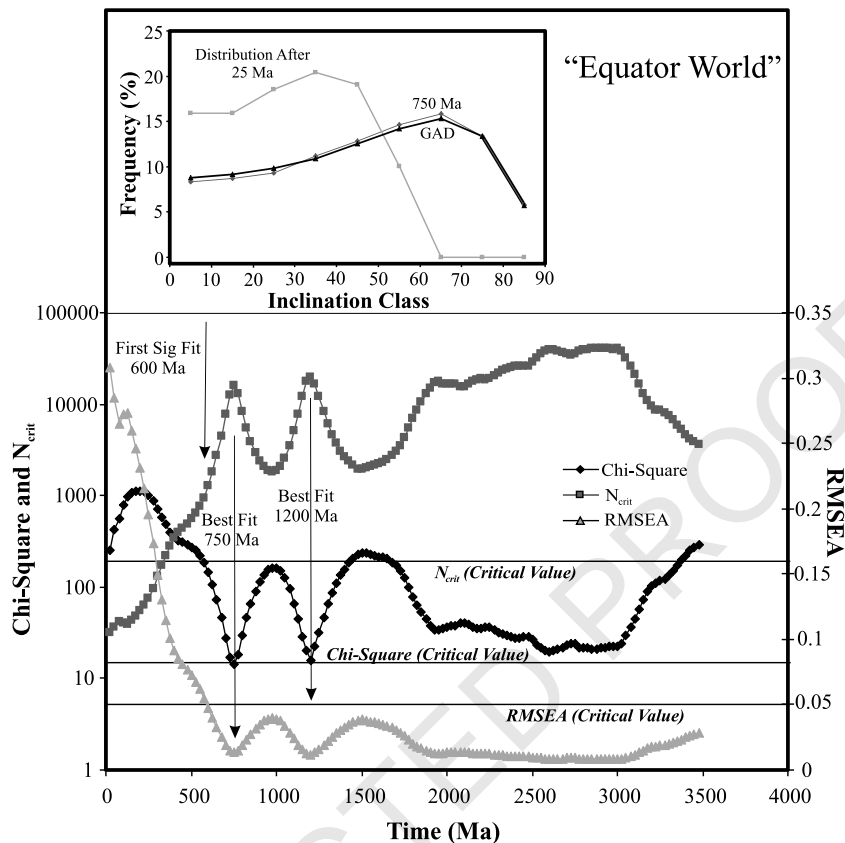


1 Fig. 5. Statistical results of a 3500 Myr run of 'cap world'. In this run, the model reaches a GAD fit after 1475 Myr and a best
 2 fit to the GAD model at 3025 Myr. The critical value for each statistical index is indicated by a labeled line. (Inset) The inclina-
 3 tion class–frequency curves for 'cap world' after 25 Myr and 1475 Myr compared to the expected GAD frequency.

Table 2
 Results from selected random walks

Run	Time (Ma)	χ^2 value	N_{crit}	RMSEA	Number of samples
Cap world-3500	1475	668	1004	0.0471	43 070
Cap world-3500	2050	479	1944	0.0338	59 860
Cap world-575	600	2077	153	0.137	17 520
Equator world-3500	600	144	931	0.0476	8 640
<i>Equator world-3500</i>	<i>750</i>	<i>14.2</i>	<i>11 796</i>	<i>0.0134</i>	<i>10 800</i>
Equator world-3500	1200	18.2	14 693	0.012	17 280
Equator world-575	600	660	743	0.062	8 640
Today world-3500	725	486	943	0.0485	29 522
Today world-3500	1 125	39.9	17 807	0.011	45 810
Today world-575a	575	3 403	108	0.144	23 414
<i>Today world-575b</i>	<i>325</i>	<i>11.5 < /C ></i>	<i>18 940</i>	<i>0.011</i>	<i>14 044</i>

14 Number of samples is equivalent to the number of 5° bins sampled in the modeled run. Bold indicates that no significant result
 15 was achieved in the run. Italics indicates all three measures of significance were achieved in the run.

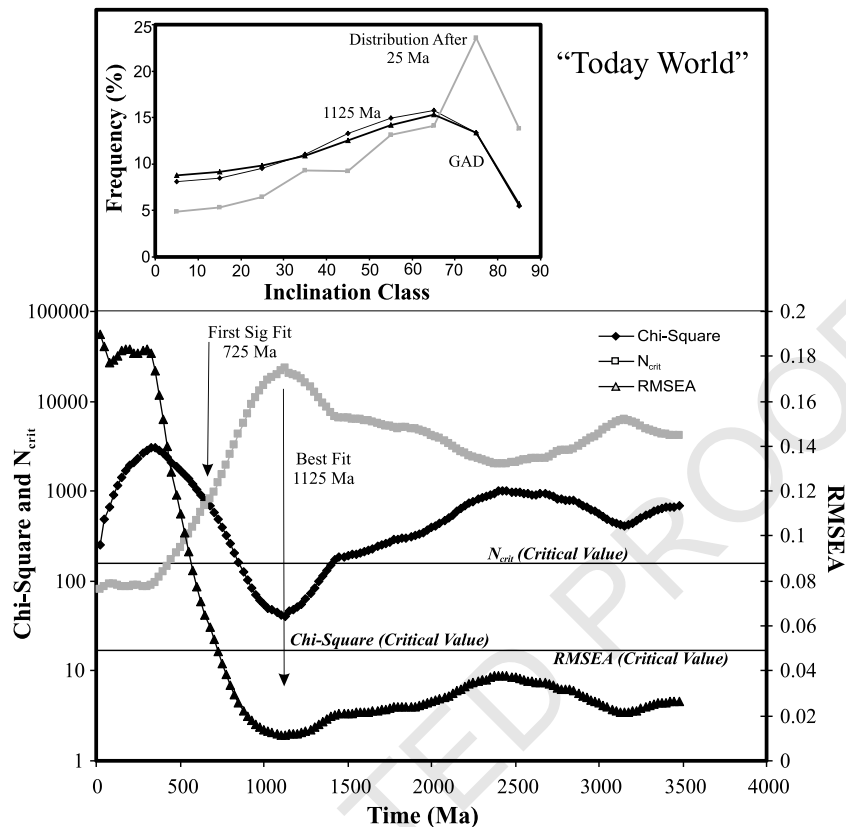


1 Fig. 6. Statistical results of a 3500 Myr run of 'equator world'. In this run, the model reaches a GAD fit after 600 Myr and a
 2 best fit to the GAD model at 750 and 1200 Myr. The critical value for each statistical index is indicated by a labeled line. (Inset)
 3 The inclination class–frequency curves for 'cap world' after 25 Myr and 750 Myr compared to the expected GAD frequency.

309 Fig. 8c,d shows the results of a 600 Myr run
 310 using the equator world starting configuration.
 311 The conditions were identical to the cap world
 312 run discussed above. The model does not generate
 313 a statistically valid fit to the GAD model (Fig. 8c)
 314 and the 'best fit' obtained after 600 Myr shows a
 315 low inclination bias (Fig. 8d, Table 2).

316 Fig. 9 shows two runs of 'today world' using
 317 identical conditions to those cited above. The only
 318 difference between the two runs was the choice of
 319 the initial random seed value and hence Euler
 320 pole sequence (see Appendix 1b). In the first ex-
 321 ample, the model does not reach a statistically
 322 valid fit after 600 Myr (Fig. 9a) and the best fit
 323 shows a high inclination bias (Fig. 9b, Table 2).
 324 In the second run, the model reaches a statistically
 325 valid fit after only 325 Myr (Fig. 9c,d; Table 2).

326 We note that in the case of the 600 Myr runs, 326
 327 the models appear sensitive to the starting condi- 327
 328 tions in that the endpoint distribution at 600 Myr 328
 329 most often reflects the initial bias. For example, 329
 330 both 'cap world' and 'today world' tend to show a 330
 331 bias towards high inclinations consistent with their 331
 332 initial biases towards high inclinations (see 332
 333 Figs. 5b and 7b). Similarly, 'equator world' tends 333
 334 to exhibit a low-latitude bias consistent with its 334
 335 starting distribution (Fig. 8c). However, this is 335
 336 not always the case. For example, Fig. 10a shows 336
 337 a cap world run most closely resembling a pure g_2^0 337
 338 or pure g_3^0 contribution. Fig. 10b shows a run of 338
 339 today world with a low inclination bias best fit to 339
 340 a 6% +G3 contribution and Fig. 10c shows an 340
 341 equator world run with a high inclination bias. 341

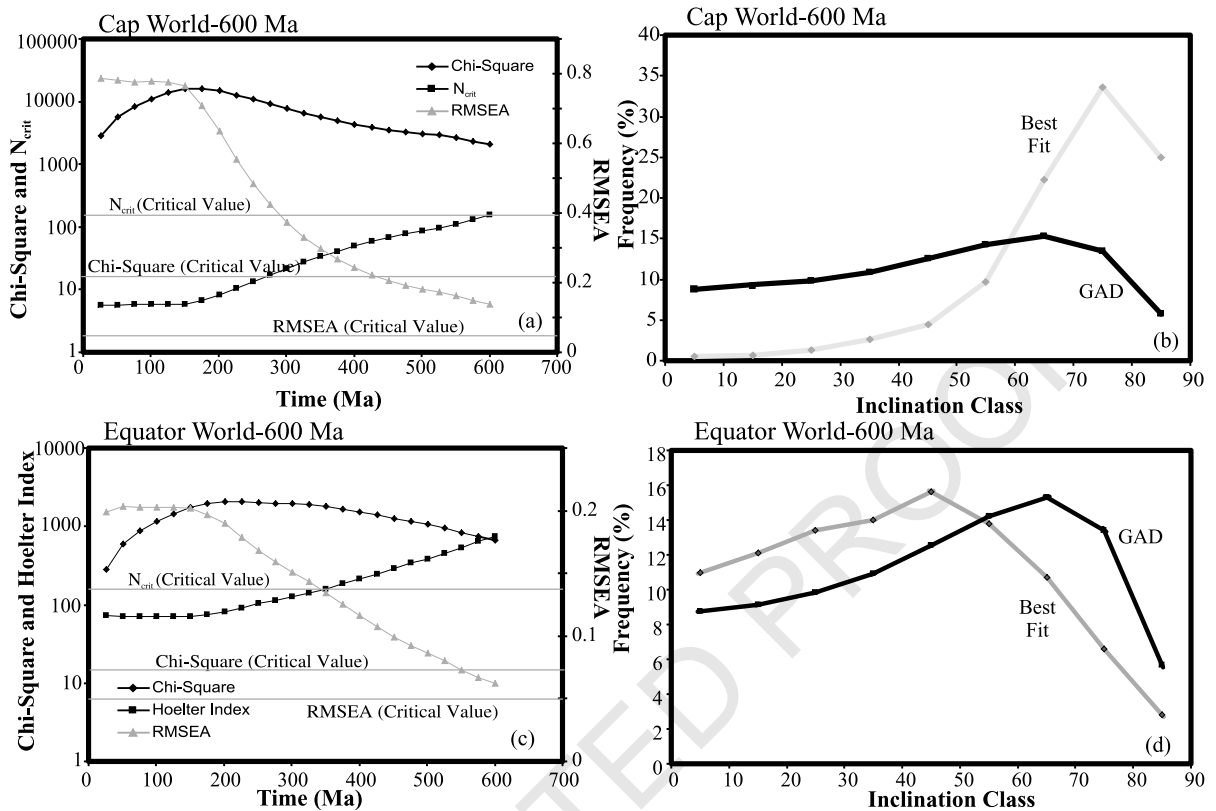


1 Fig. 7. Statistical results of a 3500 Myr run of 'today world'. In this run, the model reaches a GAD fit after 725 Myr and a best
 2 fit to the GAD model at 1125 Myr. The critical value for each statistical index is indicated by a labeled line. (Inset) The inclina-
 3 tion class–frequency curves for 'cap world' after 25 Myr and 1000 Myr compared to the expected GAD frequency.

342 4.5. Small sample sizes

343 The previously cited analyses generate much
 344 larger sample sizes than are available in the pa-
 345 leomagnetic database. We wished to examine
 346 whether or not a much smaller random sample
 347 size would be capable of testing the GAD hypoth-
 348 esis. For example, in the analysis conducted by
 349 [3], the Cenozoic database ($n = 253$ bins) yielded
 350 an inclination distribution that is statistically in-
 351 distinguishable from GAD as did the original
 352 study of the Phanerozoic by [6]. In the first case,
 353 the Cenozoic compilation of [3] represents the ef-
 354 fects of distributed sampling sites across the globe
 355 rather than a randomization process resulting
 356 from continental motion. In the second case [6],
 357 the compiled database represents results through
 358 1971. A majority of those results were not subject

to detailed demagnetization such that the influ- 359
 ence of younger overprints produced additional 360
 bias in that analysis. The maximum bin size for 361
 Mesozoic and Paleozoic times can be calculated 362
 using the 10 time periods (Cambrian–Cretaceous) 363
 multiplied by the number of $10^\circ \times 10^\circ$ bins. This 364
 calculation shows that [3] sampled only $\sim 11\%$ of 365
 the potential bins. We therefore created a set of 366
 synthetic continents covering 11% of the Earth 367
 and conducted sampling at 25 Myr intervals for 368
 485 Myr in order to mimic the Mesozoic–Paleo- 369
 zoic conditions of [3]. The model never ap- 370
 proached a GAD fit in 50+ runs, but showed a 371
 wide variety of inclination bias. 372

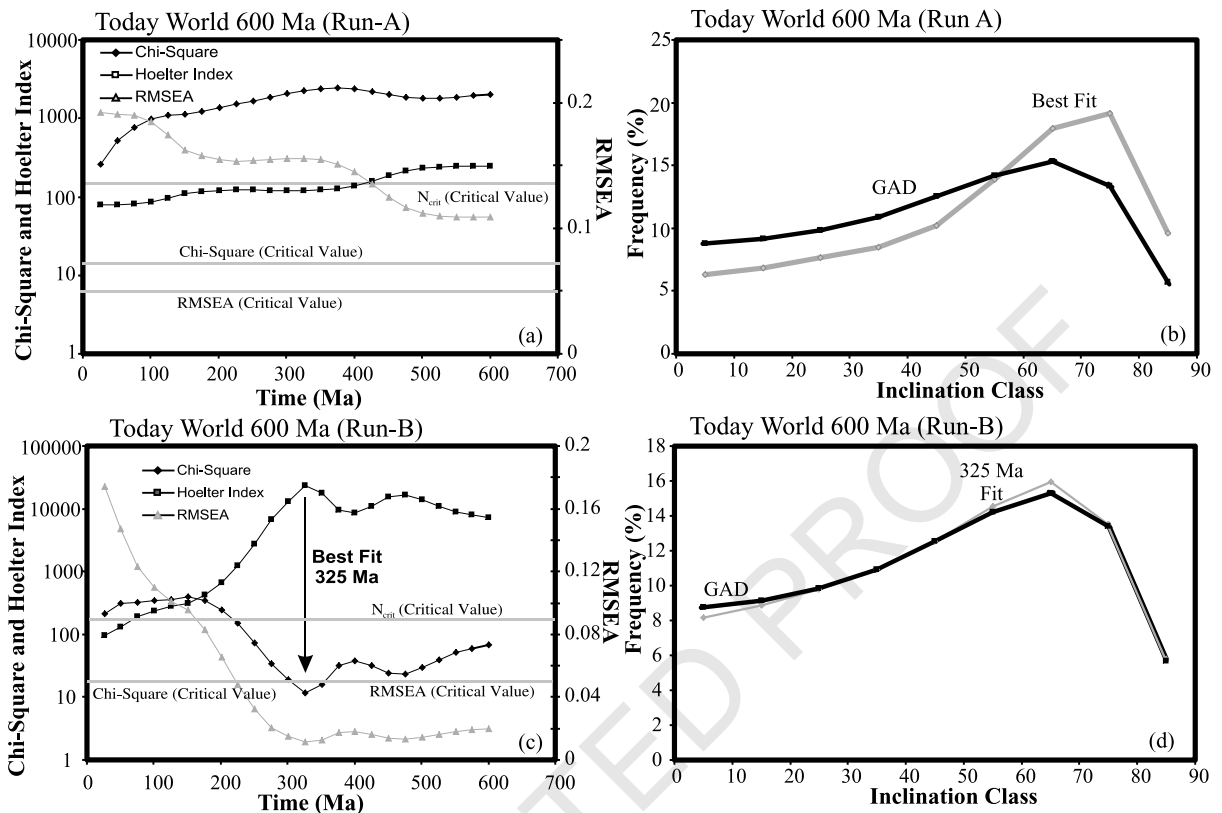


1 Fig. 8. (a) Statistical results of a 600 Myr run of 'cap world'. In this run, the model never reaches a statistically significant
 2 GAD-like fit. (b) The best fit reached after 600 Myr shows a high inclination bias for the 'cap world' run. (c) Statistical results
 3 of a 600 Myr run of 'equator world'. In this run, the model never reaches a statistically significant GAD-like fit. (d) The best fit
 4 reached after 600 Myr shows a low inclination bias for the 'equator world' run.

373 5. Discussion

374 Of the myriad explanations given for the low
 375 inclination bias observed in previous studies of
 376 inclination only data [3,7], the possibility of in-
 377 complete sampling has not been rigorously ex-
 378 plored. Our random walk model, discussed above,
 379 suggests that the previous inclination only studies
 380 are fundamentally flawed. Further, we suggest
 381 that all conclusions drawn from these earlier stud-
 382 ies should be viewed with extreme caution. We
 383 offer two principal reasons for rejecting this type
 384 of study. In an effort to determine the minimum
 385 number of studies necessary to confidently test the
 386 dipole nature of the field using inclination only
 387 studies, we ran the 'today world' model through
 388 1000 iterations. The model parameters were iden-
 389 tical to those described in Section 3.4. In the 600

390 Myr time period, the model produced inclination
 391 distributions that were statistically indistinguish-
 392 able from the GAD 29.6% of the time. To first
 393 order, this means that a 600 Myr sampling inter-
 394 val has less than a 30% chance of adequately test-
 395 ing the GAD model when properly sampled. Fur-
 396 thermore, Fig. 11 shows a histogram based on the
 397 number of bins needed to achieve a GAD-like fit.
 398 The minimum number of sampling bins needed to
 399 achieve a GAD-like fit ($5 \times 5^\circ$) was 5500. The
 400 average was 15270 bins. These numbers are par-
 401 ticularly striking when compared to previous
 402 studies. Kent and Smethurst [3] used 531 bins to
 403 evaluate the Precambrian (550–3500 Ma). The
 404 bins were based on $10^\circ \times 10^\circ$ regions and 50
 405 Myr intervals. If we consider that continental re-
 406 gions composed, on average, 25% of the surface
 407 area of the Earth during the Precambrian [16],



1 Fig. 9. (a) Statistical results of a 600 Myr run of ‘today world’. In this run, the model never reaches a statistically significant
 2 GAD-like fit. (b) The best fit reached after 600 Myr shows a high inclination bias for the ‘today world’ run. (c) Statistical results
 3 of a 600 Myr run of ‘today world’ using a different random seed. In this run, the model reaches a GAD-like fit after 225 Myr
 4 and a best fit after 325 Myr. (d) Comparison of the 325 Myr inclination–frequency curve to the GAD curve for the ‘today world’
 5 run in panel c.

408 then the theoretical maximum sample size would
 409 total 10450 bins. Thus, the study by [3] would
 410 optimistically have sampled only $\sim 5\%$ of the po-
 411 tential bins and therefore is unlikely to provide a
 412 good test of the GAD hypothesis. The Paleozoic
 413 dataset of [3] contained 352 bins averaged over
 414 300 Myr. When we ran our synthetic drift model
 415 (using 12216 bins) at 300 Myr intervals, we pro-
 416 duced a GAD-like result less than 8% of the time.
 417 The entire Phanerozoic data from [3] are more
 418 robust, with 947 total bins. Nevertheless, we esti-
 419 mate that this represents only $\sim 13\%$ of the po-
 420 tential sample size and therefore is unlikely to
 421 provide a strong test of the GAD hypothesis
 422 due to both the relatively small sample size and
 423 the short interval of time available for sampling.

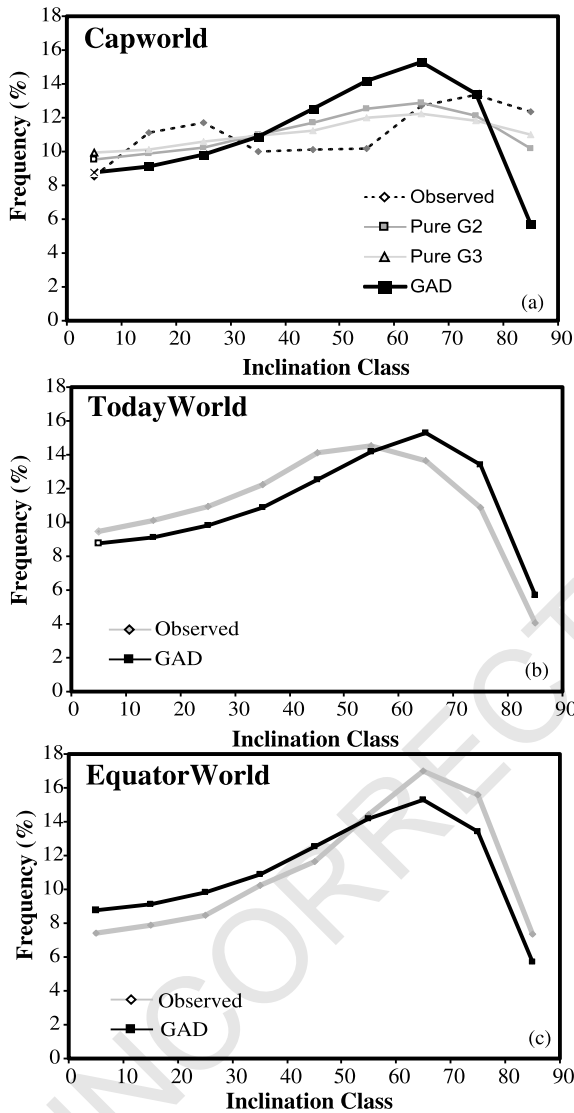
424 It is more difficult to statistically evaluate the

approach taken by [7] since our model is based on 425
 the premise of binned data. However, we note 426
 that when the corrected χ^2 values were calculated 427
 along with the N_{crit} and RMSEA statistical pa- 428
 rameters, the results were all statistically different 429
 from the GAD model. In essence, [7] was operat- 430
 ing with a slightly smaller dataset than [3]. Given 431
 that we have shown the analysis of [3] is faulty, it 432
 is difficult to imagine a scenario whereby an un- 433
 binned analysis is a superior model. 434

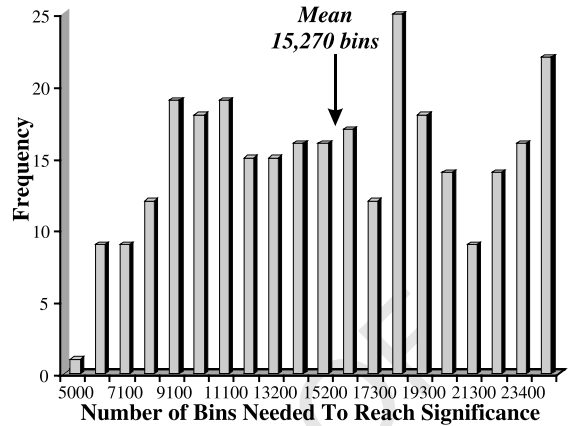
6. Conclusions 435

Previous studies that have attempted to look at 436
 inclination only distributions to test the GAD hy- 437
 pothesis were based on the assumption that 600 438

439 Myr was an adequate time period to produce a
 440 random sampling of the globe. That assumption
 441 was never tested and recent studies [3] suggested
 442 that the Paleozoic and Precambrian were domi-



1 Fig. 10. (a) Inclination class–frequency curve from a 575
 2 Myr run of ‘cap world’. In this run, the statistical best fit
 3 after 575 Myr resembles either a pure G2 or pure G3 curve.
 4 (b) Inclination class–frequency curve from a 575 Myr run of
 5 ‘today world’. In this run, the statistical best fit after 575
 6 Myr yields a low inclination bias best fit to a 6% G3 (octu-
 7 polar) field. (c) Inclination class–frequency curve from a 575
 8 Myr run of ‘equator world’. In this run, the statistical best
 9 fit after 575 Myr shows a high inclination bias.



1 Fig. 11. Histogram representing the significant results of
 2 1000 runs of ‘today world’ as sample bin size. The duration
 3 of each of these runs was 600 Myr using the parameters
 4 cited in the text. In this test, the model reached a GAD-like
 5 distribution 29.6% of the time. The average number of bins
 6 needed to reach GAD was 15270 ($5^\circ \times 5^\circ$ bins).

443 nated by modest contributions from persistent
 444 G2 (quadrupolar) and G3 (octupolar) fields. We
 445 tested the ‘random paleogeographic sampling’ as-
 446 sumption using a random walk model under a
 447 variety of conditions and configurations. Our re-
 448 sults indicate that the sampling density required
 449 to adequately test the GAD model is not attain-
 450 able using the extant paleomagnetic database.
 451 Our random walk models show that many non-
 452 GAD-like distributions can be produced via insuf-
 453 ficient sampling. Thus, previous conclusions re-
 454 garding persistent non-dipole fields based on in-
 455 clination only studies should be viewed with
 456 extreme caution. Unfortunately, the model cannot
 457 a priori test whether or not such non-dipole
 458 fields existed in the past. Indeed, other modes of anal-
 459 ysis have made the case for persistent non-dipole
 460 fields in Paleozoic–Mesozoic time [4,5] and these
 461 and other methods of GAD analysis should be
 462 pursued.

Acknowledgements

463
 464 The authors wish to thank Dennis Kent for
 465 supplying us with his binned dataset and Larry
 466 Winner (University of Florida Statistics) for inter-
 467 esting discussions on the random walk model and

468 the statistical analysis described in this paper.
 469 Trond Torsvik and Mike McElhinny are thanked
 470 for their extremely positive reviews of this paper.
 471 We also thank an anonymous reviewer for valua-
 472 ble comments. [SK]

473 Appendix 1a. Statistical tests

474 The χ^2 test compares the difference between the
 475 observed distributions and the theoretical GAD
 476 distribution and generates a χ^2 value. This value
 477 is then compared to the critical χ^2 value at the
 478 desired level of significance. A value of χ^2 which
 479 is less than the critical value signifies that the ob-
 480 served distribution cannot be distinguished from
 481 the theoretical distribution [10]. The formula for
 482 the χ^2 test is given as:

$$483 \chi^2 = \sum_{i=1}^k \frac{(O_i - E_i)^2}{E_i} \quad (A)$$

484 where O_i = observed frequency in counts and E_i is
 485 the expected frequency in counts. The analysis
 486 conducted by [3,7] mistakenly used frequency in
 487 percent which has the effect of underestimating
 488 the χ^2 value by a factor of:

$$489 O_i/100 \quad (B)$$

490 Corrected χ^2 values are given in Table 1. Un-
 491 fortunately, the χ^2 statistic is extremely sensitive
 492 to the number of observations. In a practical
 493 sense, this means that distributions based on a
 494 large N will almost always cause the χ^2 value to
 495 exceed the critical value even when the distribu-
 496 tion functions are nearly identical (see Fig. 5b;
 497 Table 2). Statisticians have therefore developed a
 498 number of additional statistical tests that are de-
 499 signed to account for the sample size used in the
 500 χ^2 analysis [11,12].

501 The Hoelster index [11] is used to evaluate the
 502 observed distribution when the χ^2 value is deemed
 503 significant. This critical N index is sensitive to the
 504 number of observations used in the analysis. The
 505 Index is calculated as follows:

$$506 N_{\text{crit}} = \frac{(N-1) \times \chi_{\text{crit}}^2}{\chi^2} + 1 \quad (C)$$

507 where N = number of observations, χ_{crit}^2 is the crit-

ical value of the χ^2 analysis and χ^2 is the calcu- 508
 lated χ^2 value from Eq. A above. N_{crit} is therefore 509
 the maximum sample size at which the χ^2 value 510
 would not be significant. Hoelster [11] recommends 511
 values of at least 200 and states that values of less 512
 than 75 indicate very poor model fit. As originally 513
 formulated, the Hoelster index should only be used 514
 to evaluate models where the χ^2 values are signifi- 515
 cant. However, we note that when the analysis is 516
 conducted on a sample distribution where the χ^2 517
 value is not significant then N_{crit} exceeds the true 518
 N used in the analysis. Thus, the Hoelster index 519
 generates useful information even when applied to 520
 statistically insignificant χ^2 distributions. 521

522 The RMSEA [12–14] is based on the non-cen-
 523 trality parameter and can be evaluated as follows:

$$524 \text{RMSEA} = \sqrt{\left[\left(\frac{\chi^2}{\text{df}-1} \right) / (N-1) \right]} \quad (D)$$

525 where df = degrees of freedom, N = number of ob-
 526 servations and χ^2 is the calculated χ^2 value from
 527 Eq. A above. Values of RMSEA < 0.05 are con-
 528 sidered an excellent fit although values of
 529 RMSEA < 0.08 are considered adequate [12,14].

530 In our analysis, we examined each of our runs
 531 and looked for statistically good fits based on at
 532 least two of the above mentioned parameters. The
 533 Hoelster index was deemed useful even when the
 534 calculated χ^2 value was not significant because it
 535 produces a peak in the N_{crit} parameter. We there-
 536 fore look for minima in both the χ^2 value and the
 537 RMSEA and maxima in the Hoelster index to as-
 538 sess our goodness of fit.

539 Appendix 1b. Randomization of Euler poles

540 We have modified the standard linear con-
 541 gruential (SLC) random number generator [15]
 542 in order to produce ‘true’ randomizing effect.
 543 Each run begins with the input of a number be-
 544 tween 0 and 655 (the range is arbitrary) to ‘seed’
 545 the random number generator. The ‘seed’ number
 546 will generate the same sequence of ‘random num-
 547 bers’ in most computer systems using the SLC
 548 formula. Our algorithm begins the run with this
 549 seed and when a new Euler pole is called for, the

550 program seeks the next sequential value in the
 551 series of random numbers. Following this, the
 552 program is ‘re-seeded’ using a random choice
 553 from one of the first 50 longitude values in the
 554 model. This has the practical effect of generating a
 555 sequence of truly random drift models. The utility
 556 of this method is that the algorithm can be ‘reset’
 557 by quitting the program and starting over with
 558 the same random seed. This allows us to test the
 559 sensitivity of the model to changing input param-
 560 eters.

561 References

- 562 [1] M.W. McElhinny, P.L. McFadden, R.T. Merrill, The
 563 time-averaged paleomagnetic field 0–5 Ma, *J. Geophys.*
 564 *Res.* 101 (1996) 25007–25027.
- 565 [2] T. Hatakeyama, M. Kono, Geomagnetic field model for
 566 the last 5 myr: time averaged field and secular variation,
 567 *Phys. Earth Planet. Inter.* 133 (2002) 181–215.
- 568 [3] D.V. Kent, M.A. Smethurst, Shallow bias of paleomag-
 569 netic inclinations in the Paleozoic and Precambrian, *Earth*
 570 *Planet. Sci. Lett.* 160 (1998) 391–402.
- 571 [4] T.H. Torsvik, R. Van der Voo, Refining Gondwana and
 572 Pangea palaeogeography; estimates of Phanerozoic non-
 573 dipole (octupole) fields, *Geophys. J. Int.* 151 (2002) 771–
 574 794.
- 575 [5] R. Van der Voo, T.H. Torsvik, Evidence for Permian and
 576 Mesozoic non-dipole fields provides an explanation for
 577 Pangea reconstruction problems, *Earth Planet. Sci. Lett.*
 578 187 (2001) 71–81.
- 579 [6] M.E. Evans, Test of the non-dipole nature of the geo-
 580 magnetic field throughout Phanerozoic time, *Nature* 262
 581 (1976) 676–677.
- [7] J.D.A. Piper, S. Grant, A paleomagnetic test of the axial
 dipole assumption and implications for continental distri-
 bution through geologic time, *Phys. Earth Planet. Inter.*
 55 (1989) 37–53.
- [8] R. Hollerbach, C.A. Jones, On the magnetically stabiliz-
 ing role of the Earth’s inner core, *Phys. Earth Planet.*
Inter. 87 (1995) 171–181.
- [9] M.W. McElhinny, P.L. McFadden, *Paleomagnetism Con-
 tinentals and Oceans*, Academic Press International Geo-
 physics Series 73, Boston, MA, 2000, 386 pp.
- [10] J.R. Carr, *Numerical Analysis for the Geological Scien-
 ces*, Prentice Hall, Englewood Cliffs, NJ, 1995, pp. 104–
 106.
- [11] J.W. Hoelter, The analysis of covariance structures, *Soc.*
Methods Res. 11 (1983) 325–344.
- [12] R. Cudeck, M.W. Browne, Constructing a covariance ma-
 trix that yields a specified minimizer and a specified mini-
 mum discrepancy function value, *Psychometrika* (1992)
 357–369.
- [13] L. Hu, P.M. Bentler, Evaluating model fit, in: R.H. Hoyle
 (Ed.), *Structural Equation Modeling: Concepts, Issues
 and Applications*, Sage Publishing, Thousand Oaks, CA,
 1995, pp. 76–99.
- [14] J. Nevitt, G.R. Hancock, Improving the root mean square
 error of approximation for nonnormal conditions in
 structural equation modeling, *J. Exp. Educ.* 68 (2000)
 251–268.
- [15] W.H. Press, B.P. Flannery, S.A. Teukolsky, W.T. Vetter-
 ing, *Numerical Recipes: The Art of Scientific Computing*,
 Cambridge University Press, Cambridge, MA, 1988, pp.
 191–225.
- [16] A. Reymer, G. Schubert, Phanerozoic addition rates to
 the continental crust and crustal growth, *Tectonics* 3
 (1984) 63–77.

582
583
584
585
586
587
588
589
590
591
592
593
594
595
596
597
598
599
600
601
602
603
604
605
606
607
608
609
610
611
612
613
614
615
616